Editors' Suggestion

Edge States and Topological Invariants of Non-Hermitian Systems

Shunyu Yao[1] and Zhong Wang[1,2,*]
[1]Institute for Advanced Study, Tsinghua University, Beijing 100084, China
[2]Collaborative Innovation Center of Quantum Matter, Beijing 100871, China

(Received 6 March 2018; published 21 August 2018)

The bulk-boundary correspondence is among the central issues of non-Hermitian topological states. We show that a previously overlooked "non-Hermitian skin effect" necessitates redefinition of topological invariants in a generalized Brillouin zone. The resultant phase diagrams dramatically differ from the usual Bloch theory. Specifically, we obtain the phase diagram of the non-Hermitian Su-Schrieffer-Heeger model, whose topological zero modes are determined by the non-Bloch winding number instead of the Bloch-Hamiltonian-based topological number. Our work settles the issue of the breakdown of conventional bulk-boundary correspondence and introduces the non-Bloch bulk-boundary correspondence.

DOI: 10.1103/PhysRevLett.121.086803

Introduction.—Topological materials are characterized by robust boundary states immune to perturbations [1–5]. According to the principle of bulk-boundary correspondence, the existence of boundary states is dictated by the bulk topological invariants, which, in the band-theory framework, are defined in terms of the Bloch Hamiltonian. The Hamiltonian is often assumed to be Hermitian. In many physical systems, however, non-Hermitian Hamiltonians [6,7] are more appropriate. For example, they are widely used in describing open systems [8–17], wave systems with gain and loss [18–40] (e.g., photonic and acoustic [41–44]), and solid-state systems where electron-electron interactions or disorders introduce a non-Hermitian self-energy into the effective Hamiltonian of quasiparticle [45–47]. With these physical motivations, there have recently been growing efforts, both theoretically [48–78] and experimentally [79–85], to investigate topological phenomena of non-Hermitian Hamiltonians.

Among the key issues is the fate of bulk-boundary correspondence in non-Hermitian systems. Recently, numerical results in a one-dimensional (1D) model show that open-boundary spectra look quite different from periodic-boundary ones, which seems to indicate a complete breakdown of bulk-boundary correspondence [49,86]. In view of this breakdown, a possible scenario is that the topological edge states depend on all sample details, without any general rule telling their existence or absence. Here, we ask the following questions: Is there a generalized bulk-boundary correspondence? Are there bulk topological invariants responsible for the topological edge states? Affirmative answers are obtained in this Letter.

We start from solving a 1D model. Interestingly, all the eigenstates of an open chain are found to be localized near the boundary (dubbed the "non-Hermitian skin effect"), in contrast to the extended Bloch waves in Hermitian cases. In the simplest situations, this effect can be understood in terms of an imaginary gauge field [87,88]. We show that the non-Hermitian skin effect has dramatic consequences in establishing a "non-Bloch bulk-boundary correspondence" in which the topological boundary modes are determined by "non-Bloch topological invariants".

Previous non-Hermitian topological invariants [48–56] are formulated in terms of the Bloch Hamiltonian. The crucial non-Bloch-wave nature of eigenstates (non-Hermitian skin effect) is untouched; therefore, the number of topological edge modes is not generally related to these topological invariants. In view of the non-Hermitian skin effect, we introduce a non-Bloch topological invariant, which faithfully determines the number of topological edge modes. It embodies the non-Bloch bulk-boundary correspondence of non-Hermitian systems.

Model.—The non-Hermitian Su-Schrieffer-Heeger (SSH) model [89,90] is pictorially shown in Fig. 1. Related models are relevant to quite a few experiments [79,82,92]. The Bloch Hamiltonian is

$$H(k) = d_x\sigma_x + \left(d_y + i\frac{\gamma}{2}\right)\sigma_y, \tag{1}$$

where $d_x = t_1 + (t_2 + t_3)\cos k$, $d_y = (t_2 - t_3)\sin k$, and $\sigma_{x,y}$ are the Pauli matrices. A mathematically equivalent model was studied in Ref. [49], where σ_y was replaced by σ_z; as such, the physical interpretation was not SSH. The model

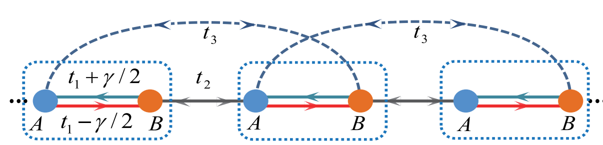

FIG. 1. Non-Hermitian SSH model. The dotted box indicates the unit cell.

has a chiral symmetry [3] $\sigma_z^{-1}H(k)\sigma_z = -H(k)$, which ensures that the eigenvalues appear in $(E, -E)$ pairs: $E_\pm(k) = \pm\sqrt{d_x^2 + (d_y + i\gamma/2)^2}$. Let us first take $t_3 = 0$ for simplicity (nonzero t_3 will be included later). The energy gap closes at the exceptional points $(d_x, d_y) = (\pm\gamma/2, 0)$, which requires $t_1 = t_2 \pm \gamma/2$ $(k = \pi)$ or $t_1 = -t_2 \pm \gamma/2$ $(k = 0)$.

The open-boundary spectrum is noticeably different from that of the periodic boundary [49,93], which can be seen in the numerical spectra of real-space Hamiltonian of an open chain (Fig. 2). The zero modes are robust to perturbation [Fig. 2(d)], which indicates their topological origin. A transition point is located at $t_1 \approx 1.20$, which is a quite unremarkable point from the perspective of $H(k)$ whose spectrum is gapped there ($|E_\pm(k)| \neq 0$). As such, the topology of $H(k)$ cannot determine the zero modes, which challenges the familiar Hermitian wisdom. The question arises: What topological invariant predicts the zero modes?

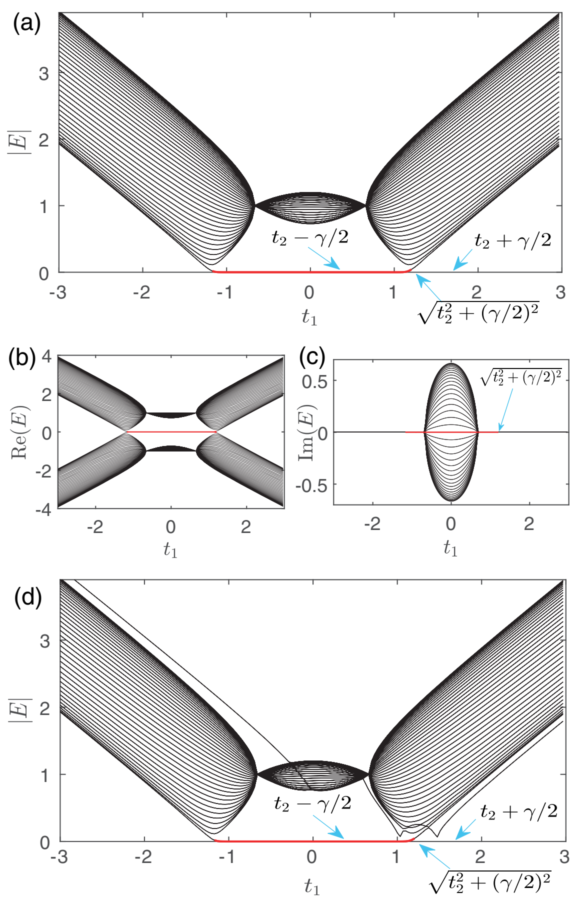

FIG. 2. Numerical spectra of an open chain with length $L = 40$ (unit cell). $t_2 = 1$, $\gamma = 4/3$; t_1 varies in $[-3, 3]$. (a) $|E|$ as functions of t_1. The zero-mode line is shown in red (twofold degenerate, ignoring an indiscernible split). The true transition point $[\sqrt{t_2^2 + (\gamma/2)^2} \approx 1.20]$ and the $H(k)$-gap-closing points $(t_2 \pm \gamma/2)$ are indicated by arrows. (b),(c) The real and imaginary parts of E. (d) The same as (a) except that the value of t_1 at the leftmost bond is replaced by $t_1 - 0.8$, which generates additional nonzero modes, but the zero modes are unaffected.

Shortcut solution.—To gain insights, we analytically solve an open chain. The wave function is written as $|\psi\rangle = (\psi_{1,A}, \psi_{1,B}, \psi_{2,A}, \psi_{2,B}, \ldots, \psi_{L,A}, \psi_{L,B})^T$. We first present a shortcut, which is applicable only to the $t_3 = 0$ case. The real-space eigenequation $H|\psi\rangle = E|\psi\rangle$ is equivalent to $\bar{H}|\bar{\psi}\rangle = E|\bar{\psi}\rangle$ with $|\bar{\psi}\rangle = S^{-1}|\psi\rangle$ and

$$\bar{H} = S^{-1}HS. \tag{2}$$

We can judiciously choose S in this similarity transformation. Let us take S to be a diagonal matrix whose diagonal elements are $\{1, r, r, r^2, r^2, \ldots, r^{L-1}, r^{L-1}, r^L\}$, then in $\bar{H}$ we have $r^{\pm1}(t_1 \pm \gamma/2)$ in the place of $t_1 \pm \gamma/2$ (Fig. 1). If we take $r = \sqrt{|(t_1 - \gamma/2)/(t_1 + \gamma/2)|}$, $\bar{H}$ becomes the standard SSH model for $|t_1| > |\gamma/2|$, with intracell and intercell hoppings

$$\bar{t}_1 = \sqrt{(t_1 - \gamma/2)(t_1 + \gamma/2)}, \qquad \bar{t}_2 = t_2. \tag{3}$$

The k-space expression is

$$\bar{H}(k) = (\bar{t}_1 + \bar{t}_2 \cos k)\sigma_x + \bar{t}_2 \sin k\sigma_y. \tag{4}$$

The transition points are $\bar{t}_1 = \bar{t}_2$, namely,

$$t_1 = \pm\sqrt{t_2^2 + (\gamma/2)^2}. \tag{5}$$

For the parameters in Fig. 2, Eq. (5) gives $t_1 \approx \pm1.20$. Note that any $H(k)$-based topological invariants [48–56] can jump only at $t_1 = \pm t_2 \pm \gamma/2$, where the gap of $H(k)$ closes.

A bulk eigenstate $|\bar{\psi}_l\rangle$ of Hermitian $\bar{H}$ is extended; therefore, H's eigenstate $|\psi_l\rangle = S|\bar{\psi}_l\rangle$ is exponentially localized at an end of the chain when $\gamma \neq 0$. It implies that the usual Bloch phase factor e^{ik} is replaced by $\beta \equiv re^{ik}$ in the open-boundary system (i.e., the wave vector acquires an imaginary part: $k \to k - i\ln r$). Although this intuitive picture is based on the shortcut solution, we believe that the exponential-decay behavior of eigenstates (non-Hermitian skin effect) is a general feature of non-Hermitian bands.

Generalizable solution.—The intuitive shortcut solution has limitations; e.g., it is inapplicable when $t_3 \neq 0$. Here, we rederive the solution in a more generalizable way (still focusing on $t_3 = 0$ for simplicity). The real-space eigen-equation leads to $t_2\psi_{n-1,B} + [t_1 + (\gamma/2)]\psi_{n,B} = E\psi_{n,A}$ and $[t_1 - (\gamma/2)]\psi_{n,A} + t_2\psi_{n+1,A} = E\psi_{n,B}$ in the bulk of chain. We take the ansatz that $|\psi\rangle = \sum_j |\phi^{(j)}\rangle$, where each $|\phi^{(j)}\rangle$ takes the exponential form (omitting the j index temporarily): $(\phi_{n,A}, \phi_{n,B}) = \beta^n(\phi_A, \phi_B)$, which satisfies

$$\left[\left(t_1+\frac{\gamma}{2}\right)+t_2\beta^{-1}\right]\phi_B=E\phi_A,$$
$$\left[\left(t_1-\frac{\gamma}{2}\right)+t_2\beta\right]\phi_A=E\phi_B. \tag{6}$$

Therefore, we have

$$\left[\left(t_1-\frac{\gamma}{2}\right)+t_2\beta\right]\left[\left(t_1+\frac{\gamma}{2}\right)+t_2\beta^{-1}\right]=E^2, \tag{7}$$

which has two solutions, namely, $\beta_{1,2}(E)=[E^2+\gamma^2/4-t_1^2-t_2^2\pm\sqrt{(E^2+\gamma^2/4-t_1^2-t_2^2)^2-4t_2^2(t_1^2-\gamma^2/4)}]/[2t_2(t_1+\gamma/2)]$, where $+(-)$ corresponds to $\beta_1(\beta_2)$. In the $E\to 0$ limit, we have

$$\beta_{1,2}^{E\to 0}=-\frac{t_1-\gamma/2}{t_2}, \qquad -\frac{t_2}{t_1+\gamma/2}. \tag{8}$$

They can also be seen from Eq. (6). These two solutions correspond to $\phi_B=0$ and $\phi_A=0$, respectively.

Restoring the j index in $|\phi^{(j)}\rangle$, we have

$$\phi_A^{(j)}=\frac{E}{t_1-\gamma/2+t_2\beta_j}\phi_B^{(j)}, \qquad \phi_B^{(j)}=\frac{E}{t_1+\gamma/2+t_2\beta_j^{-1}}\phi_A^{(j)}. \tag{9}$$

These two equations are equivalent because of Eq. (7). The general solution is written as a linear combination:

$$\begin{pmatrix}\psi_{n,A}\\ \psi_{n,B}\end{pmatrix}=\beta_1^n\begin{pmatrix}\phi_A^{(1)}\\ \phi_B^{(1)}\end{pmatrix}+\beta_2^n\begin{pmatrix}\phi_A^{(2)}\\ \phi_B^{(2)}\end{pmatrix}, \tag{10}$$

which should satisfy the boundary condition

$$\left(t_1+\frac{\gamma}{2}\right)\psi_{1,B}-E\psi_{1,A}=0,$$
$$\left(t_1-\frac{\gamma}{2}\right)\psi_{L,A}-E\psi_{L,B}=0. \tag{11}$$

Together with Eq. (9), they lead to

$$\beta_1^{L+1}(t_1-\gamma/2+t_2\beta_2)=\beta_2^{L+1}(t_1-\gamma/2+t_2\beta_1). \tag{12}$$

We are concerned about the spectrum for a long chain, which necessitates $|\beta_1|=|\beta_2|$ for the bulk eigenstates. If not, suppose that $|\beta_1|<|\beta_2|$, we would be able to discard the tiny β_1^{L+1} term in Eq. (12), and the equation becomes $\beta_2=0$ or $t_1-\gamma/2+t_2\beta_1=0$ (without the appearance of L). As a bulk-band property, $|\beta_1(E)|=|\beta_2(E)|$ remains valid in the presence of perturbations near the edges [e.g., Fig. 2(d)], and essentially determines the bulk-band energies [98]. Combined with $\beta_1\beta_2=(t_1-\gamma/2)/(t_1+\gamma/2)$ coming from Eq. (7), $|\beta_1|=|\beta_2|$ leads to

$$|\beta_j|=r\equiv\sqrt{\left|\frac{t_1-\gamma/2}{t_1+\gamma/2}\right|} \tag{13}$$

for bulk eigenstates (i.e., eigenstates in the continuum spectrum). The same r has just been used in the shortcut solution.

We emphasize that $r<1$ indicates that all the eigenstates are localized at the left end of the chain [see Fig. 3(c) for illustration] [94,96]. In Hermitian systems, the orthogonality of eigenstates excludes this non-Hermitian skin effect.

There are various ways to rederive the transition points in Eq. (5). To introduce one of them, we first plot in Fig. 3(a) the $|\beta|-E$ curve solved from Eq. (7) for $t_1=t_2=1, \gamma=4/3$. The spectrum is real for this set of parameters; therefore, no imaginary part of E is needed (This reality is related to PT symmetry [6,7]). The expected $|\beta_1|=|\beta_2|=r$ relation is found on the line

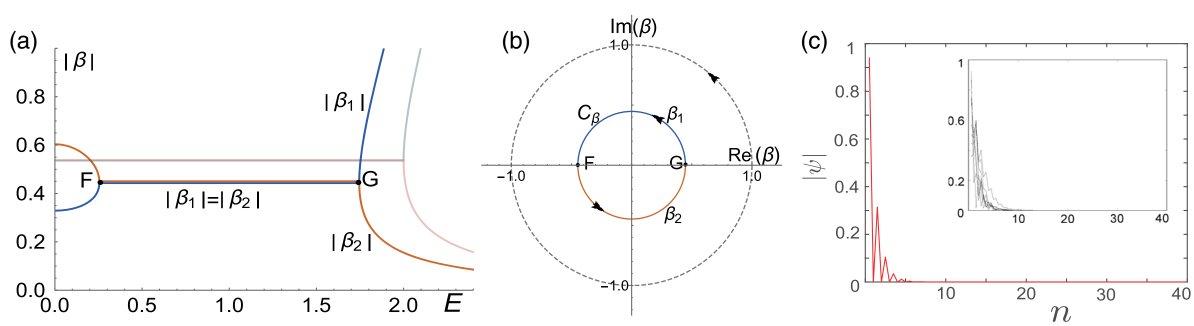

FIG. 3. (a) $|\beta_j|-E$ curves from Eq. (7). $t_1=1$ (dark color) and $\sqrt{t_2^2+(\gamma/2)^2}\approx 1.20$ (light color). (b) Complex-valued β_j's form a closed loop C_β, which is a circle for the present model [by Eq. (13)]. The shown one is for $t_1=1$. C_β can be viewed as a deformed Brillouin zone that generalizes the usual one. In Hermitian cases, C_β is a unit circle (dashed line). (c) Profile of a zero mode (main figure) and eight randomly chosen bulk eigenstates (inset), illustrating the non-Hermitian skin effect found in the analytic solution, namely, all the bulk eigenstates are localized near the boundary. $t_1=1$. Common parameters: $t_2=1, \gamma=4/3$.

FG [Fig. 3(a)], which is associated with bulk spectra. As t_1 is increased from 1, F moves towards the left, and finally hits the $|\beta|$ axis ($E = 0$ axis). Apparently, it occurs when $|\beta_1^{E\to 0}| = |\beta_2^{E\to 0}| = r$. Inserting Eq. (8) into this equation, we have

$$t_1 = \pm\sqrt{t_2^2 + (\gamma/2)^2} \quad \text{or} \quad \pm\sqrt{-t_2^2 + (\gamma/2)^2}. \tag{14}$$

At these points, the open-boundary continuum spectra touch zero energy, enabling topological transitions.

A simpler way to rederive Eq. (5) is to calculate the open-boundary spectra. According to Eq. (13), we can take $\beta = re^{ik}$ ($k \in [0, 2\pi]$) in Eq. (7) to obtain the spectra,

$$E^2(k) = t_1^2 + t_2^2 - \gamma^2/4 + t_2\sqrt{|t_1^2 - \gamma^2/4|}[\mathrm{sgn}(t_1 + \gamma/2)e^{ik} + \mathrm{sgn}(t_1 - \gamma/2)e^{-ik}], \tag{15}$$

which recovers the spectrum of SSH model when $\gamma = 0$. The spectra are real when $|t_1| > |\gamma|/2$. Equation (14) can be readily rederived as the gap-closing condition of Eq. (15) ($|E(k)| = 0$).

Before proceeding, we comment on a subtle issue in the standard method of finding zero modes. For concreteness, let us consider the present model, and focus on zero modes at the left end of a long chain. One can see that $|\psi^{\mathrm{zero}}\rangle$ with $(\psi_{n,A}^{\mathrm{zero}}, \psi_{n,B}^{\mathrm{zero}}) = (\beta_1^{E\to 0})^n(1, 0)$ appears as a zero-energy eigenstate [see Eq. (8) for $\beta_1^{E\to 0}$]. In the standard approach, the normalizable condition $|\beta_1^{E\to 0}| < 1$ is imposed, and the transition points satisfy $|\beta_1^{E\to 0}| = 1$, which predicts $t_1 = t_2 + \gamma/2$ as a transition point, being consistent with the gap closing of $H(k)$. Such an apparent but misleading consistency has hidden the true transition points and topological invariants in quite a few previous studies of non-Hermitian models. The implicit assumption was that the bulk eigenstates are extended Bloch waves with $|\beta| = 1$, into which the zero modes merge at transitions. In reality, the bulk eigenstates have $|\beta| = r$ (eigenstate skin effect); therefore, the true merging-into-bulk condition is

$$|\beta_1^{E\to 0}| = r, \tag{16}$$

which correctly produces $t_1 = \sqrt{t_2^2 + (\gamma/2)^2}$. This is a manifestation of the non-Bloch bulk-boundary correspondence.

Non-Bloch topological invariant.—The bulk-boundary correspondence is fulfilled if we can find a bulk topological invariant that determines the edge modes. Previous constructions take $H(k)$ as the starting point [48–56], which should be revised in view of the non-Hermitian skin effect. The usual Bloch waves carry a pure phase factor e^{ik}, whose role is now played by β. In addition to the phase factor, β has a modulus $|\beta| \neq 1$ in general [e.g., Eq. (13)]. Therefore, we start from the non-Bloch Hamiltonian obtained from $H(k)$ by the replacement $e^{ik} \to \beta, e^{-ik} \to \beta^{-1}$:

$$H(\beta) = \left(t_1 - \frac{\gamma}{2} + \beta t_2\right)\sigma_- + \left(t_1 + \frac{\gamma}{2} + \beta^{-1} t_2\right)\sigma_+, \tag{17}$$

where $\sigma_\pm = (\sigma_x \pm i\sigma_y)/2$. We have taken $t_3 = 0$ for simplicity. As explained in both the shortcut and generalizable solutions, β takes values in a nonunit circle $|\beta| = r$ (in other words, k acquires an imaginary part $-i\ln r$). It is notable that the open-boundary spectra in Eq. (15) are given by $H(\beta)$ instead of $H(k)$. The right and left eigenvectors are defined by

$$H(\beta)|u_R\rangle = E(\beta)|u_R\rangle, \quad H^\dagger(\beta)|u_L\rangle = E^*(\beta)|u_L\rangle. \tag{18}$$

Chiral symmetry ensures that $|\tilde{u}_R\rangle \equiv \sigma_z|u_R\rangle$ and $|\tilde{u}_L\rangle \equiv \sigma_z|u_L\rangle$ is also right and left eigenvector, with eigenvalues $-E$ and $-E^*$, respectively. In fact, one can diagonalize the matrix as $H(\beta) = TJT^{-1}$ with $J = \begin{pmatrix} E & \\ & -E \end{pmatrix}$, then each column of T and $(T^{-1})^\dagger$ is a right and left eigenvector, respectively, and the normalization condition $\langle u_L|u_R\rangle = \langle\tilde{u}_L|\tilde{u}_R\rangle = 1, \langle u_L|\tilde{u}_R\rangle = \langle\tilde{u}_L|u_R\rangle = 0$ is guaranteed. As a generalization of the usual "Q matrix" [3], we define

$$Q(\beta) = |\tilde{u}_R(\beta)\rangle\langle\tilde{u}_L(\beta)| - |u_R(\beta)\rangle\langle u_L(\beta)|, \tag{19}$$

which is off-diagonal due to the chiral symmetry $\sigma_z^{-1}Q\sigma_z = -Q$, namely, $Q = \begin{pmatrix} & q \\ q^{-1} & \end{pmatrix}$. Now we introduce the non-Bloch winding number:

$$W = \frac{i}{2\pi}\int_{C_\beta} q^{-1}dq. \tag{20}$$

Crucially, it is defined on the "generalized Brillouin zone" C_β [Fig. 3(b)]. It is useful to mention that the conventional formulations using $H(k)$ may sometimes produce correct phase diagrams, if C_β happens to be a unit circle [97].

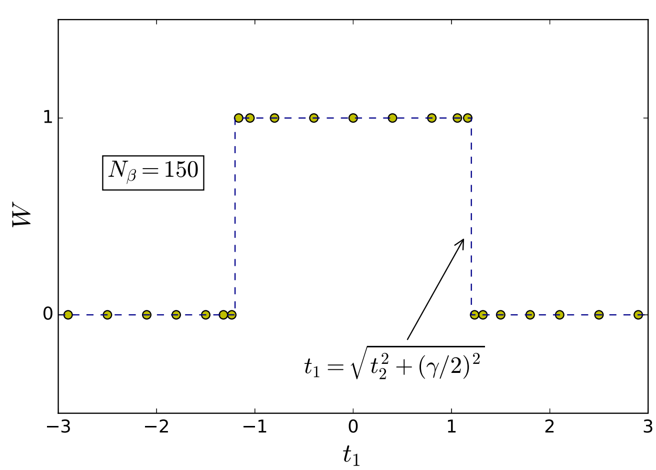

FIG. 4. Numerical result of topological invariant. N_β is the number of grid points on C_β. $t_2 = 1, \gamma = 4/3$.

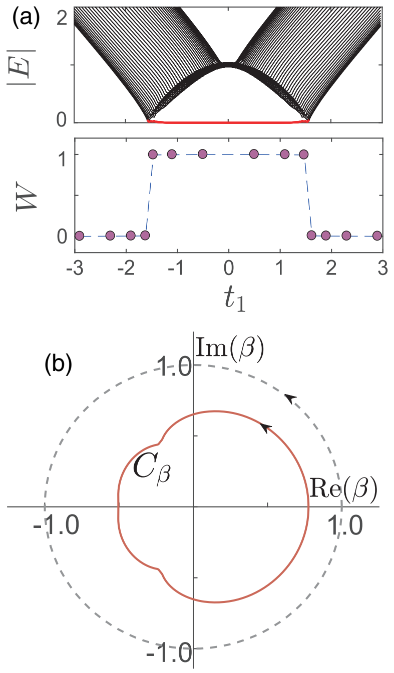

FIG. 5. The nonzero t_3 case. (a) Upper panel: Spectrum of an open chain; $t_2 = 1, \gamma = 4/3, t_3 = 1/5$; $L = 100$. Lower panel: topological invariant calculated using 200 grid points on C_β. The transition points are $t_1 \approx \pm 1.56$. (b) C_β for $t_1 = 1.1$.

The numerical results for $t_3 = 0$ is shown in Fig. 4, which is consistent with the analytical spectra obtained above. Quantitatively, $2W$ counts the total number of robust zero modes at the left and right ends. For example, corresponding to Fig. 2, there are two zero modes for $t_1 \in [-\sqrt{t_2^2 + (\gamma/2)^2}, \sqrt{t_2^2 + (\gamma/2)^2}]$, and none elsewhere. The analytic solution shows that, for $[t_2 - \gamma/2, \sqrt{t_2^2 + (\gamma/2)^2}]$, both modes live at the left end, for $[-t_2 + \gamma/2, t_2 - \gamma/2]$, one for each end, and for $[-\sqrt{t_2^2 + (\gamma/2)^2}, -t_2 + \gamma/2]$, both at the right end. Thus, the $H(k)$-gap closing points $\pm(t_2 - \gamma/2)$ are where zero modes migrate from one end to the other, conserving the total mode number. In fact, one can see $|\beta_{j=1\,\mathrm{or}\,2}^{E\to 0}| = 1$ at $\pm(t_2 - \gamma/2)$, indicating the penetration into bulk.

To provide a more generic exemplification, we take a nonzero t_3. Now we find [98] that C_β is no longer a circle (bulk eigenstates with different energies have different $|\beta|$), yet $2W$ correctly predicts the total zero-mode number (Fig. 5).

Finally, we remarked that Eq. (20) can be generalized to multiband systems. Each pair of bands (labeled by l) possesses a $C_\beta^{(l)}$ curve, and the Q matrix [Eq. (19)] becomes $Q^{(l)}$, each one defining a winding number $W^{(l)}$ (with matrix trace). The topological invariant is $W = \sum_l W^{(l)}$.

Conclusions.—Through the analytic solution of non-Hermitian SSH model, we explained why the usual bulk-boundary correspondence breaks down, and how the non-Bloch bulk-boundary correspondence takes its place. Two of the key concepts are the non-Hermitian skin effect and generalized Brillouin zone. We formulate the generalized bulk-boundary correspondence by introducing a precise topological invariant that faithfully predicts the topological edge modes. The physics presented here can be generalized to a rich variety of non-Hermitian systems, which will be left for future studies.

This work is supported by NSFC under Grant No. 11674189.

*wangzhongemail@gmail.com

[1] M. Z. Hasan and C. L. Kane, Colloquium: Topological insulators, Rev. Mod. Phys. **82**, 3045 (2010).
[2] X.-L. Qi and S.-C. Zhang, Topological insulators and superconductors, Rev. Mod. Phys. **83**, 1057 (2011).
[3] C.-K. Chiu, J. C. Y. Teo, A. P. Schnyder, and S. Ryu, Classification of topological quantum matter with symmetries, Rev. Mod. Phys. **88**, 035005 (2016).
[4] B. A. Bernevig and T. L. Hughes, *Topological Insulators and Topological Superconductors* (Princeton University Press, Princeton, NJ, 2013).
[5] A. Bansil, H. Lin, and T. Das, Colloquium: Topological band theory, Rev. Mod. Phys. **88**, 021004 (2016).
[6] C. M. Bender and S. Boettcher, Real Spectra in Non-Hermitian Hamiltonians Having *PT* Symmetry, Phys. Rev. Lett. **80**, 5243 (1998).
[7] C. M. Bender, Making sense of non-Hermitian Hamiltonians, Rep. Prog. Phys. **70**, 947 (2007).
[8] I. Rotter, A non-Hermitian Hamilton operator and the physics of open quantum systems, J. Phys. A **42**, 153001 (2009).
[9] S. Malzard, C. Poli, and H. Schomerus, Topologically Protected Defect States in Open Photonic Systems with Non-Hermitian Charge-Conjugation and Parity-Time Symmetry, Phys. Rev. Lett. **115**, 200402 (2015).
[10] H. J. Carmichael, Quantum Trajectory Theory for Cascaded Open Systems, Phys. Rev. Lett. **70**, 2273 (1993).
[11] B. Zhen, C. W. Hsu, Y. Igarashi, L. Lu, I. Kaminer, A. Pick, S.-L. Chua, J. D. Joannopoulos, and M. Soljačić, Spawning rings of exceptional points out of dirac cones, Nature (London) **525**, 354 (2015).
[12] S. Diehl, E. Rico, M. A. Baranov, and P. Zoller, Topology by dissipation in atomic quantum wires, Nat. Phys. **7**, 971 (2011).
[13] H. Cao and J. Wiersig, Dielectric microcavities: Model systems for wave chaos and non-Hermitian physics, Rev. Mod. Phys. **87**, 61 (2015).
[14] Y. Choi, S. Kang, S. Lim, W. Kim, J.-R. Kim, J.-H. Lee, and K. An, Quasieigenstate coalescence in an atom-cavity quantum composite, Phys. Rev. Lett. **104**, 153601 (2010).
[15] P. San-Jose, J. Cayao, E. Prada, and R. Aguado, Majorana bound states from exceptional points in non-topological superconductors, Sci. Rep. **6**, 21427 (2016).
[16] T. E. Lee and C.-K. Chan, Heralded Magnetism in Non-Hermitian Atomic Systems, Phys. Rev. X **4**, 041001 (2014).

[17] T. E. Lee, F. Reiter, and N. Moiseyev, Entanglement and Spin Squeezing in Non-Hermitian Phase Transitions, Phys. Rev. Lett. **113**, 250401 (2014).

[18] K. G. Makris, R. El-Ganainy, D. N. Christodoulides, and Z. H. Musslimani, Beam Dynamics in $\mathcal{PT}$ Symmetric Optical Lattices, Phys. Rev. Lett. **100**, 103904 (2008).

[19] S. Longhi, Bloch Oscillations in Complex Crystals with $\mathcal{PT}$ Symmetry, Phys. Rev. Lett. **103**, 123601 (2009).

[20] S. Klaiman, U. Günther, and N. Moiseyev, Visualization of Branch Points in $\mathcal{PT}$-Symmetric Waveguides, Phys. Rev. Lett. **101**, 080402 (2008).

[21] A. Regensburger, C. Bersch, M.-A. Miri, G. Onishchukov, D. N. Christodoulides, and U. Peschel, Parity-time synthetic photonic lattices, Nature (London) **488**, 167 (2012).

[22] S. Bittner, B. Dietz, U. Günther, H. L. Harney, M. Miski-Oglu, A. Richter, and F. Schäfer, Pt-Symmetry and Spontaneous Symmetry Breaking in a Microwave Billiard, Phys. Rev. Lett. **108**, 024101 (2012).

[23] C. E. Rüter, K. G. Makris, R. El-Ganainy, D. N. Christodoulides, M. Segev, and D. Kip, Observation of parity-time symmetry in optics, Nat. Phys. **6**, 192 (2010).

[24] Z. Lin, H. Ramezani, T. Eichelkraut, T. Kottos, H. Cao, and D. N. Christodoulides, Unidirectional invisibility induced by $\mathcal{PT}$-symmetric periodic structures, Phys. Rev. Lett. **106**, 213901 (2011).

[25] L. Feng, Y.-L. Xu, W. S. Fegadolli, M.-H. Lu, J. E. B. Oliveira, V. R. Almeida, Y.-F. Chen, and A. Scherer, Experimental demonstration of a unidirectional reflectionless parity-time metamaterial at optical frequencies, Nat. Mater. **12**, 108 (2013).

[26] A. Guo, G. J. Salamo, D. Duchesne, R. Morandotti, M. Volatier-Ravat, V. Aimez, G. A. Siviloglou, and D. N. Christodoulides, Observation of $\mathcal{PT}$-Symmetry Breaking in Complex Optical Potentials, Phys. Rev. Lett. **103**, 093902 (2009).

[27] M. Liertzer, L. Ge, A. Cerjan, A. D. Stone, H. E. Türeci, and S. Rotter, Pump-Induced Exceptional Points in Lasers, Phys. Rev. Lett. **108**, 173901 (2012).

[28] B. Peng, Ş. K. Özdemir, S. Rotter, H. Yilmaz, M. Liertzer, F. Monifi, C. M. Bender, F. Nori, and L. Yang, Loss-induced suppression and revival of lasing, Science **346**, 328 (2014).

[29] R. Fleury, D. Sounas, and A. Alù, An invisible acoustic sensor based on parity-time symmetry, Nat. Commun. **6**, 5905 (2015).

[30] L. Chang, X. Jiang, S. Hua, C. Yang, J. Wen, L. Jiang, G. Li, G. Wang, and M. Xiao, Parity–time symmetry and variable optical isolation in active–passive-coupled microresonators, Nat. Photonics **8**, 524 (2014).

[31] H. Hodaei, A. U. Hassan, S. Wittek, H. Garcia-Gracia, R. El-Ganainy, D. N. Christodoulides, and M. Khajavikhan, Enhanced sensitivity at higher-order exceptional points, Nature (London) **548**, 187 (2017).

[32] H. Hodaei, M.-A. Miri, M. Heinrich, D. N. Christodoulides, and M. Khajavikhan, Parity-time–symmetric microring lasers, Science **346**, 975 (2014).

[33] L. Feng, Z. J. Wong, R.-M. Ma, Y. Wang, and X. Zhang, Single-mode laser by parity-time symmetry breaking, Science **346**, 972 (2014).

[34] T. Gao, E. Estrecho, K. Y. Bliokh, T. C. H. Liew, M. D. Fraser, S. Brodbeck, M. Kamp, C. Schneider, S. Höfling, Y. Yamamoto *et al.*, Observation of non-hermitian degeneracies in a chaotic exciton-polariton billiard, Nature (London) **526**, 554 (2015).

[35] H. Xu, D. Mason, L. Jiang, and J. G. E. Harris, Topological energy transfer in an optomechanical system with exceptional points, Nature (London) **537**, 80 (2016).

[36] Y. Ashida, S. Furukawa, and M. Ueda, Parity-time-symmetric quantum critical phenomena, Nat. Commun. **8**, 15791 (2017).

[37] K. Kawabata, Y. Ashida, and M. Ueda, Information retrieval and criticality in parity-time-symmetric systems, Phys. Rev. Lett. **119**, 190401 (2017).

[38] W. Chen, Ş. K. Özdemir, G. Zhao, J. Wiersig, and L. Yang, Exceptional points enhance sensing in an optical microcavity, Nature (London) **548**, 192 (2017).

[39] K. Ding, G. Ma, M. Xiao, Z. Q. Zhang, and C. T. Chan, Emergence, Coalescence, and Topological Properties of Multiple Exceptional Points and their Experimental Realization, Phys. Rev. X **6**, 021007 (2016).

[40] C. A. Downing and G. Weick, Topological collective plasmons in bipartite chains of metallic nanoparticles, Phys. Rev. B **95**, 125426 (2017).

[41] T. Ozawa, H. M. Price, A. Amo, N. Goldman, M. Hafezi, L. Lu, M. Rechtsman, D. Schuster, J. Simon, O. Zilberberg, and I. Carusotto, Topological Photonics, arXiv:1802.04173.

[42] L. Lu, J. D. Joannopoulos, and M. Soljacic, Topological photonics, Nat. Photonics **8**, 821 (2014).

[43] R. El-Ganainy, K. G. Makris, M. Khajavikhan, Z. H. Musslimani, S. Rotter, and D. N. Christodoulides, Non-Hermitian physics and pt symmetry, Nat. Phys. **14**, 11 (2018).

[44] S. Longhi, Parity-Time Symmetry meets Photonics: A New Twist in non-Hermitian Optics, arXiv:1802.05025.

[45] V. Kozii and L. Fu, Non-Hermitian Topological Theory of Finite-Lifetime Quasiparticles: Prediction of Bulk Fermi Arc due to Exceptional Point, arXiv:1708.05841.

[46] M. Papaj, H. Isobe, and L. Fu, Bulk Fermi arc of disordered Dirac fermions in two dimensions, arXiv:1802.00443.

[47] H. Shen and L. Fu, Quantum Oscillation from In-Gap States and Non-Hermitian Landau Level Problem, Phys. Rev. Lett. **121**, 026403 (2018).

[48] K. Esaki, M. Sato, K. Hasebe, and M. Kohmoto, Edge states and topological phases in non-Hermitian systems, Phys. Rev. B **84**, 205128 (2011).

[49] T. E. Lee, Anomalous edge state in a non-Hermitian lattice, Phys. Rev. Lett. **116**, 133903 (2016).

[50] D. Leykam, K. Y. Bliokh, C. Huang, Y. D. Chong, and F. Nori, Edge Modes, Degeneracies, and Topological Numbers in non-Hermitian Systems, Phys. Rev. Lett. **118**, 040401 (2017).

[51] H. Menke and M. M. Hirschmann, Topological quantum wires with balanced gain and loss, Phys. Rev. B **95**, 174506 (2017).

[52] S. Lieu, Topological phases in the non-Hermitian Su-Schrieffer-Heeger model, Phys. Rev. B **97**, 045106 (2018).

[53] H. Shen, B. Zhen, and L. Fu, Topological Band Theory for Non-Hermitian Hamiltonians, Phys. Rev. Lett. **120**, 146402 (2018).

[54] C. Yin, H. Jiang, L. Li, R. Lü, and S. Chen, Geometrical meaning of winding number and its characterization of topological phases in one-dimensional chiral non-Hermitian systems, Phys. Rev. A **97**, 052115 (2018).

[55] C. Li, X. Z. Zhang, G. Zhang, and Z. Song, Topological phases in a kitaev chain with imbalanced pairing, Phys. Rev. B **97**, 115436 (2018).

[56] M. S. Rudner and L. S. Levitov, Topological transition in a non-Hermitian quantum walk, Phys. Rev. Lett. **102**, 065703 (2009).

[57] S.-D. Liang and G.-Y. Huang, Topological invariance and global berry phase in non-Hermitian systems, Phys. Rev. A **87**, 012118 (2013).

[58] Y. C. Hu and T. L. Hughes, Absence of topological insulator phases in non-Hermitian pt-symmetric Hamiltonians, Phys. Rev. B **84**, 153101 (2011).

[59] Z. Gong, S. Higashikawa, and M. Ueda, Zeno Hall Effect, Phys. Rev. Lett. **118**, 200401 (2017).

[60] J. Gong and Q.-h. Wang, Geometric phase in $\mathcal{PT}$-symmetric quantum mechanics, Phys. Rev. A **82**, 012103 (2010).

[61] M. S. Rudner, M. Levin, and L. S. Levitov, Survival, decay, and topological protection in non-Hermitian quantum transport, arXiv:1605.07652.

[62] K. Kawabata, Y. Ashida, H. Katsura, and M. Ueda, Parity-Time-Symmetric Topological Superconductor, Phys. Rev. B **98**, 085116 (2018).

[63] X. Ni, D. Smirnova, A. Poddubny, D. Leykam, Y. Chong, and A. B. Khanikaev, Exceptional points in topological edge spectrum of PT symmetric domain walls, arXiv:1801.04689.

[64] A. A. Zyuzin and A. Y. Zyuzin, Flat band in disorder-driven non-Hermitian Weyl semimetals, Phys. Rev. B **97**, 041203 (2018).

[65] A. Cerjan, M. Xiao, L. Yuan, and S. Fan, Effects of non-Hermitian perturbations on Weyl Hamiltonians with arbitrary topological charges, Phys. Rev. B **97**, 075128 (2018).

[66] L. Zhou, Q.-h. Wang, H. Wang, and J. Gong, Dynamical quantum phase transitions in non-Hermitian lattices, arXiv:1711.10741.

[67] J. González and R. A. Molina, Topological protection from exceptional points in Weyl and nodal-line semimetals, Phys. Rev. B **96**, 045437 (2017).

[68] M. Klett, H. Cartarius, D. Dast, J. Main, and G. Wunner, Relation between $\mathcal{PT}$-symmetry breaking and topologically nontrivial phases in the Su-Schrieffer-Heeger and Kitaev models, Phys. Rev. A **95**, 053626 (2017).

[69] M. Klett, H. Cartarius, D. Dast, J. Main, and G. Wunner, Topological edge states in the Su-Schrieffer-Heeger model subject to balanced particle gain and loss, arXiv:1802.06128.

[70] C. Yuce, Majorana edge modes with gain and loss, Phys. Rev. A **93**, 062130 (2016).

[71] C. Yuce, Topological phase in a non-Hermitian PT symmetric system, Phys. Lett. A **379**, 1213 (2015).

[72] Y. Xu, S.-T. Wang, and L.-M. Duan, Weyl exceptional rings in a three-dimensional dissipative cold atomic gas, Phys. Rev. Lett. **118**, 045701 (2017).

[73] W. Hu, H. Wang, P. P. Shum, and Y. D. Chong, Exceptional points in a non-Hermitian topological pump, Phys. Rev. B **95**, 184306 (2017).

[74] X. Wang, T. Liu, Y. Xiong, and P. Tong, Spontaneous $\mathcal{PT}$-symmetry breaking in non-Hermitian Kitaev and extended Kitaev models, Phys. Rev. A **92**, 012116 (2015).

[75] S. Ke, B. Wang, H. Long, K. Wang, and P. Lu, Topological edge modes in non-Hermitian plasmonic waveguide arrays, Opt. Express **25**, 11132 (2017).

[76] N. X. A. Rivolta, H. Benisty, and B. Maes, Topological edge modes with $\mathcal{PT}$ symmetry in a quasiperiodic structure, Phys. Rev. A **96**, 023864 (2017).

[77] Z. Gong, Y. Ashida, K. Kawabata, K. Takasan, S. Higashikawa, and M. Ueda, Topological phases of non-Hermitian systems, arXiv:1802.07964v1.

[78] G. Harari, M. A. Bandres, Y. Lumer, M. C. Rechtsman, Y. D. Chong, M. Khajavikhan, D. N. Christodoulides, and M. Segev, Topological insulator laser: Theory, Science **359**, eaar4003 (2018).

[79] J. M. Zeuner, M. C. Rechtsman, Y. Plotnik, Y. Lumer, S. Nolte, M. S. Rudner, M. Segev, and A. Szameit, Observation of a Topological Transition in the Bulk of a Non-Hermitian System, Phys. Rev. Lett. **115**, 040402 (2015).

[80] X. Zhan, L. Xiao, Z. Bian, K. Wang, X. Qiu, B. C. Sanders, W. Yi, and P. Xue, Detecting Topological Invariants in Nonunitary Discrete-Time Quantum Walks, Phys. Rev. Lett. **119**, 130501 (2017).

[81] L. Xiao, X. Zhan, Z. H. Bian, K. K. Wang, X. Zhang, X. P. Wang, J. Li, K. Mochizuki, D. Kim, N. Kawakami, W. Yi, H. Obuse, B. C. Sanders, and P. Xue, Observation of topological edge states in parity–time-symmetric quantum walks, Nat. Phys. **13**, 1117 (2017).

[82] S. Weimann, M. Kremer, Y. Plotnik, Y. Lumer, S. Nolte, K. G. Makris, M. Segev, M. C. Rechtsman, and A. Szameit, Topologically protected bound states in photonic parity–time-symmetric crystals, Nat. Mater. **16**, 433 (2017).

[83] M. Parto, S. Wittek, H. Hodaei, G. Harari, M. A. Bandres, J. Ren, M. C. Rechtsman, M. Segev, D. N. Christodoulides, and M. Khajavikhan, Complex Edge-State Phase Transitions in 1D Topological Laser Arrays, Phys. Rev. Lett. **120**, 113901 (2018).

[84] H. Zhao, P. Miao, M. H. Teimourpour, S. Malzard, R. El-Ganainy, H. Schomerus, and L. Feng, Topological hybrid silicon microlasers, Nat. Commun. **9**, 981 (2018).

[85] H. Zhou, C. Peng, Y. Yoon, C. W. Hsu, K. A. Nelson, L. Fu, J. D. Joannopoulos, M. Soljacic, and B. Zhen, Observation of bulk fermi arc and polarization half charge from paired exceptional points, Science **359**, 1009 (2018).

[86] Y. Xiong, Why does bulk boundary correspondence fail in some non-Hermitian topological models, J. Phys. Commun. **2**, 035043 (2018).

[87] S. Longhi, Nonadiabatic robust excitation transfer assisted by an imaginary gauge field, Phys. Rev. A **95**, 062122 (2017).

[88] N. Hatano and D. R. Nelson, Localization transitions in non-Hermitian quantum mechanics, Phys. Rev. Lett. **77**, 570 (1996).

[89] W. P. Su, J. R. Schrieffer, and A. J. Heeger, Soliton excitations in polyacetylene, Phys. Rev. B **22**, 2099 (1980).

[90] Related models have been studied in Refs. [52,54,91].

[91] B. Zhu, R. Lü, and S. Chen, $\mathcal{PT}$ symmetry in the non-Hermitian Su-Schrieffer-Heeger model with complex boundary potentials, Phys. Rev. A **89**, 062102 (2014).

[92] C. Poli, M. Bellec, U. Kuhl, F. Mortessagne, and H. Schomerus, Selective enhancement of topologically induced interface states in a dielectric resonator chain, Nat. Commun. **6**, 6710 (2015).

[93] We note that the numerical precision of Ref. [49] is improvable. According to our exact results, the zero-mode line in their Fig. 3(a) should span the entire $[-1/\sqrt{2}, 1/\sqrt{2}]$ interval, instead of the two disconnected lines there.

[94] Recently we noticed Ref. [95], in which similar localization is found numerically; however, in contrast to our viewpoint, it is suggested there that the localization lessens the relevance of zero modes and destroys bulk-boundary correspondence. Also note that the zero-mode interval in their Fig. 1 differs from our exact solutions.

[95] V. M. M. Alvarez, J. E. B. Vargas, and L. E. F. F. Torres, Non-Hermitian robust edge states in one dimension: Anomalous localization and eigenspace condensation at exceptional points, Phys. Rev. B **97**, 121401 (2018).

[96] We emphasize that the bulk energy spectra remain insensitive to a small perturbation at the ends of a long chain. In fact, the eigenstates of $H^\dagger$ (namely, left eigenstates) have opposite exponential decay and the outcome of a perturbation depends on the product of right and left eigenstates.

[97] For example, we find that it is the case for the model numerically studied in Ref. [52].

[98] See Supplemental Material at http://link.aps.org/supplemental/10.1103/PhysRevLett.121.086803, for details of calculation.